

Optical Absorption of CoO and MnO above and below the Néel Temperature*

G. W. PRATT, JR., *Lincoln Laboratory, Massachusetts Institute of Technology, Lexington, Massachusetts*

AND

ROLAND COELHO, *Laboratory for Insulation Research, Massachusetts Institute of Technology, Cambridge, Massachusetts*

(Received May 25, 1959)

The optical absorption of single-crystal CoO and MnO both above and below the Néel temperature is reported and interpreted. The absorption spectrum in each case is similar to that found in dilute paramagnetic salts of the same ions. Tanabe and Sugano's strong-field theory was used to interpret the data. In CoO the tetragonal distortion of the cubic lattice present in the antiferromagnetic phase was experimentally observed. An estimate of the strength of the tetragonal field is given. It is also found that the temperature dependence of the absorption coefficient in CoO is in accord with a second order electric dipole-phonon transition mechanism.

INTRODUCTION

THE oxides of the transition elements belong to a special class of materials in that the d -shell is being filled starting with the oxides of Ti and continuing to the oxides of Cu. In this series we find metals, insulators, paramagnetics, antiferromagnetics, and ferrites. Since the d -shell is incomplete, ordinary band theory would predict that the oxides would in general be metallic. Indeed TiO is a metal and V_2O_5 a metal in the paramagnetic state but a semiconductor in the antiferromagnetic phase. Generally, however, these oxides are good insulators. Thus there seem to be cases where band theory works and others in which a Heitler-London approach is more appropriate. These points have been considered by Mott,¹ Slater,² and Morin.³ Aside from the transport properties we of course have the antiferromagnetism itself to deal with. As yet there is no really good understanding of how the ordered ground state is achieved.

A study of the optical properties of these materials can provide new and significant information for a better theoretical understanding. In this paper the optical transmission of single-crystal MnO and CoO in the paramagnetic and antiferromagnetic states is reported. Both of these oxides are ionic crystals with the NaCl structure. The interpretation is based on crystal field theory or ligand field theory as developed by Orgel⁴ and Tanabe and Sugano⁵ which has so successfully described the optical properties of dilute paramagnetic salts. The philosophy behind this method is to represent the interactions between the paramagnetic ion and its surroundings by a spin-independent effective potential having the symmetry of the environment. One solves for the energy levels of the ion as perturbed by the crystal-

line field and the optical transitions are thought of as occurring between these perturbed states. Actually the crystal field must account for Coulomb interactions of the paramagnetic ion with the surrounding ions, as well as direct and indirect exchange interactions and covalent interactions with the neighbors. One of the questions that this work seeks to answer is to what extent can crystal field theory be applied to these magnetically concentrated salts and does it work equally well for the paramagnetic and antiferromagnetic states. The experimental results presented here lead to the conclusion that to within a few percent the crystal field approach does describe the optical properties in both magnetic phases. This result was not entirely unforeseen due to the success of Kanamori⁶ in his treatment based on this model of the susceptibility and anisotropy of CoO and FeO. Early optical work by Morin⁷ also pointed in this direction.

In the next section the experimental details of the work are described. Then follows the interpretation of the results for CoO and MnO. Finally a few remarks are made about the interaction of the ions and the phonons.

EXPERIMENTAL METHODS AND RESULTS

These optical transmission experiments were carried out with single-crystal MnO and CoO.⁸ Both crystals have the NaCl structure and in each case the samples were (100) planes. Thin slices were cut with a diamond saw and their thickness further reduced by grinding and polishing. The materials being very brittle, it was not possible to obtain thin samples of large area. The single MnO sample available was approximately 8×10^{-2} mm thick whereas the CoO samples were usually of 3×10^{-2} mm thickness. A 10^{-2} mm thick CoO sample was prepared and used in an unsuccessful attempt to observe the top of what appears to be the fundamental absorption edge near 4200 Å.

The samples were cemented with Canada balsam onto crystal quartz plates which made good thermal contact

* The work reported in this paper was performed by Lincoln Laboratory, a center for research operated by Massachusetts Institute of Technology with the joint support of the U. S. Army, Navy, and Air Force.

¹ N. F. Mott, Proc. Phys. Soc. (London) **A62**, 416 (1949).

² J. C. Slater, Phys. Rev. **82**, 538 (1951).

³ F. J. Morin, Bell System Tech. J. **37**, 1047 (1958).

⁴ L. E. Orgel, J. Chem. Phys. **23**, 1004 (1955).

⁵ Y. Tanabe and S. Sugano, J. Phys. Soc. (Japan) **9**, 753 (1954).

⁶ J. Kanamori, Progr. Theoret. Phys. (Kyoto) **17**, 177 (1957).

⁷ F. J. Morin, Phys. Rev. **93**, 1195 (1954).

⁸ The CoO sample was kindly supplied by Professor Nagamiya.

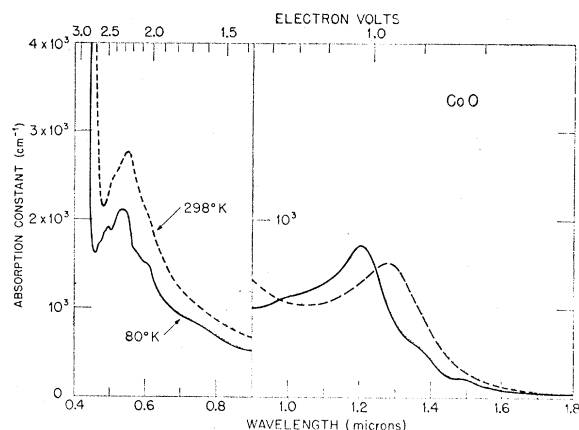


Fig. 1. Optical absorption of single crystal CoO at 298°K and 78°K. $T_N = 293^\circ\text{K}$. Note change of scale in ordinate at $\sim 0.9 \mu$.

with the cooling liquid reservoir when in position in the optical cryostat. The light beam was focused onto the sample with a 2-in. focal length quartz lens mounted outside the transmission Dewar which was fitted with CaF_2 windows. Another identical lens was used to keep the transmitted beam cylindrical.

As the absorption is smaller in the near infrared than in the visible, it was possible to use thicker and hence larger samples. Focusing of the beam and cementing of the sample, both serious sources of error in the infrared, were thus avoided. The measurements were made with standard recording spectrophotometers. A Cary 12M was used in the visible and a Beckman DK-2 in the near infrared. Both instruments can record directly the quantity $\log_{10}(I/I_0)$. In view of the small amount of transmitted energy, the slit opening could not be made smaller than 0.15 mm at 5000 Å. The corresponding resolution is of the order of 20 Å. The results obtained for MnO and CoO are shown in Figs. 1 and 2. The reflection spectrum of CoO in the visible was compared to that of aluminum so that a correction for reflection loss could be made in the transmission data. However, the accuracy of the absorption constant α is not better than roughly 25% for several reasons, chief of which is the scattering of light in the samples. Of course the point of major interest here is only the positions and structure of the absorptions.

Slices of CoO observed with a petrographic microscope were optically isotropic above the Néel point. When the sample was cooled below that point, 291°K , optical anisotropy was revealed. This was observed under crossed polarizers as a transmission pattern with areas of maximum intensity preferentially orientated along the 110 directions of the crystals. The pattern was unaffected when an external magnetic field of a few kilogauss was applied.

INTERPRETATION

The observed absorptions in both MnO and CoO can be satisfactorily explained as being due to transitions

from the ground state of the paramagnetic ion in a cubic crystalline field to higher lying Stark levels. The analysis of the results is based on the work of Tanabe and Sugano⁵ where the strong-field approximation is invoked. The cubic crystal field potential V_c does not commute with the L^2 operator of the free ion. If V_c represents a strong perturbation, the perturbed states can not even approximately be labeled in the LS representation used for the free ion. However, the perturbed states can all be labeled according to the irreducible representation of the cubic group for which they form a basis. Thus Tanabe and Sugano use the ST representation where Γ refers to an irreducible representation of O_h .

Given a free-ion configuration d^n , it is first necessary to find all of the possible ST states in the cubic field. This is done by Tanabe and Sugano as follows. The fivefold degenerate d -orbital is split by V_c into a lower lying threefold degenerate set $d\gamma$ having F_2 symmetry⁹ and a doubly degenerate pair $d\epsilon$ of E symmetry as shown in Fig. 3. As is seen from Fig. 3, the strength of the cubic field is measured by the parameter Dq . Starting from d^n in the free ion, one could now construct the states ST by combining states of $d\epsilon^m d\gamma^p$ with $m+p = n$ in much the same way that one constructs states of

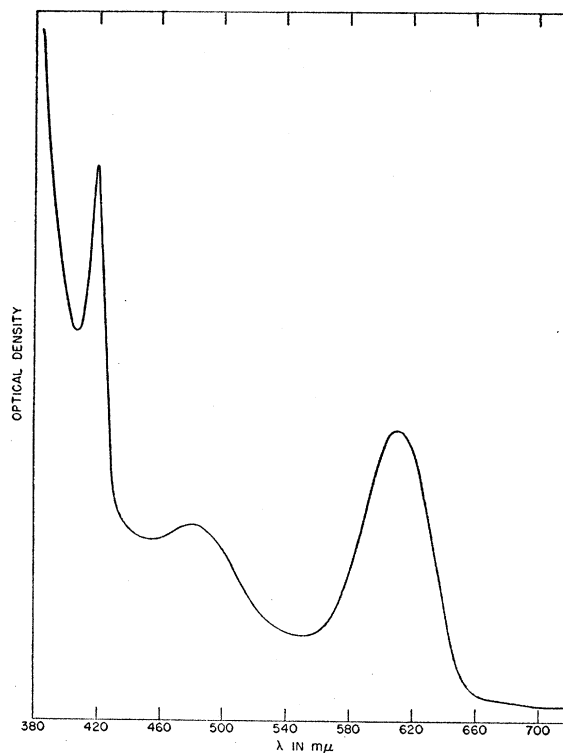


Fig. 2. Optical absorption of single crystal MnO at 78°K. $T_N = 120^\circ\text{K}$.

⁹ The representations of the cubic group are denoted here by A_1, A_2, E, F_1, F_2 . In Bethe's notation they are $\Gamma_1, \Gamma_2, \Gamma_3, \Gamma_4$, and Γ_5 , respectively.

definite angular momentum. There will be matrix components of the Hamiltonian which is $H_{\text{free ion}} + V_c$ between states of the same S and Γ . The secular equations arising from such matrix components are given by Tanabe and Sugano for all of the d^n configurations of the transition metal ions. These results will now be applied to the MnO and CoO cases. In a later section spin-orbit coupling, exchange effects, and the effect of crystal distortion will be taken up.

Co²⁺ IN A CUBIC FIELD

The level scheme for a Co²⁺ ion is shown in Fig. 4. All of the energy levels of the free ion which arise from a fixed number of d electrons can be described by just two constants B and C known as the Racah parameters¹⁰ which are related to the Slater integrals for atomic spectra by

$$B = F_2 - 5F_4,$$

and

$$C = 35F_4.$$

The way in which they enter here is shown in Fig. 4. The ground state of the free Co²⁺ is 4F which splits in a cubic field into a lowest lying 4F_1 threefold spatially degenerate level, next a 4F_2 threefold level, and above this there is the spatially nondegenerate 4A_2 level. The next state above the 4F ground level of the free ion is the 4P state which becomes a 4F_1 state in the cubic field and mixes with the 4F_1 state derived from 4F .

Only two constants Dq and B are required to fit all the quartet ($S = \frac{3}{2}$) state energies. These parameters were determined in the paramagnetic state at 298°K (the Néel temperature of CoO is 293°K) using the $^4F_1 - ^4F_2$ and $^4F_1 - ^4F_1$ transitions. According to Tanabe and Sugano the energy of the 4F_2 level is $2Dq - 15B$ and the energies of the two 4F_1 states are the roots of the 2×2

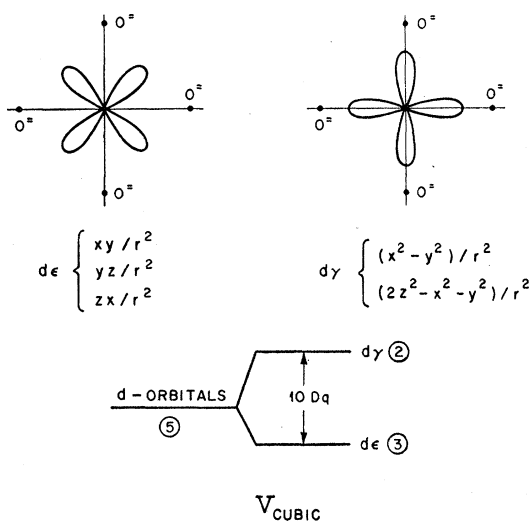


FIG. 3. Splitting of the d -orbitals by a cubic crystal field.

¹⁰ G. Racah, Phys. Rev. **62**, 438 (1942).

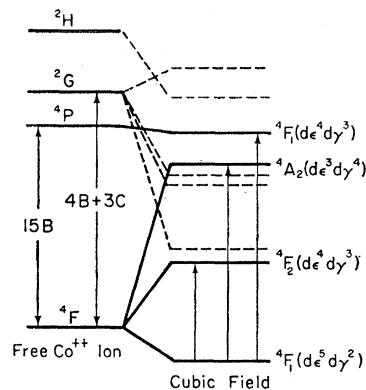


FIG. 4. Energy level scheme for the Co²⁺ ion with d^7 configuration in a cubic crystal field. Doublet states indicated by dotted lines.

secular equation given below:

$$\begin{vmatrix} 2Dq - 3B - E & 6B \\ 6B & -8Dq - 12B - E \end{vmatrix} = 0.$$

The separation of the roots of this secular equation was taken to correspond to the main absorption of CoO at room temperature which occurred at 18450 cm^{-1} . The absorption at 7810 cm^{-1} at room temperature should be the ground 4F_1 to 4F_2 transition. With this identification the value of Dq was found to be 888 cm^{-1} and B was 780 cm^{-1} . These results place the ground 4F_1 to 4A_2 transition at 16680 cm^{-1} . In Fig. 1 it will be noted that at 16130 cm^{-1} there is an indication of a very weak absorption. The relative weakness of this transition can be understood as follows. The principal configurations in terms of the $d\epsilon$ and $d\gamma$ orbitals for all of the ST levels of interest are given in Fig. 4. The 4A_2 state comes from the configuration $d\epsilon^3 d\gamma^4$ whereas the ground 4F_1 state is principally $d\epsilon^5 d\gamma^2$ with a small admixture of the $d\epsilon^4 d\gamma^3$ configuration coming from the 4P level of the free ion. Since a transition involving the change of two d -orbitals can be expected to be rather weak, the ground to 4A_2 absorption can be attributed primarily to the component of the upper 4F_1 level in the ground state. From the secular equation we find for the ground-state wave function

$$^4F_1(\text{ground}) = 0.97 ^4F_1(^4F) + 0.25 ^4F_1(^4P).$$

Hence the $^4F_1 \rightarrow ^4A_2$ transition should be roughly 0.06 as strong as the other two quartet absorptions.

Before turning to the results at 78°K for CoO we consider the role played by the doublet ($S = \frac{1}{2}$) states which are shown in Fig. 4. These states in order of increasing energy separation from the ground state are 2E , 2F_1 , 2F_2 , 2F_1 , and 2A_1 . Their energies are obtained by solving the appropriate secular equations given by Tanabe and Sugano. If the crystal field theory were to hold accurately, it would be possible to describe the positions of all these states by the parameters Dq , B , and C . Since a transition from the ground state to a doublet involves a change in multiplicity, it must proceed via a spin-dependent coupling. Therefore, we can expect that these transitions will be somewhat weaker than those to

TABLE I. The first row labeled level denotes the states corresponding to the d^7 configuration for Co^{++} in a cubic field. The second and third rows give the observed and calculated positions of these levels in cm^{-1} . The fourth row shows the results of Pappalardo for $\text{CoBr}_2 \cdot 6\text{H}_2\text{O}$. The fifth row gives Low's results for Co^{++} in MgO . In the lower part of the table the values of the parameters Dq , B , and C are given in cm^{-1} for Co^{++} in various environments.

Level	4F_2	2E	2F_1	2F_2	4A_2	4F_1	2F_1	2A_1
CoO , 78°K {obs.	7250-8333	13 000	16 340	16 560	17 240	18 250-18 780	20 080-20 660	21 010
{theo.	8333	9775	15 540	16 570	17 755	18 520	21 450	22 610
$\text{CoBr}_2 \cdot 6\text{H}_2\text{O}$, 20°K	16 200	16 490	...	18 120-18 600	19 745-20 980	21 750-24 375
Co in MgO	8470	9080	17 200	18 700	19 600	20 500	24 600	
			Dq	B	C			
Free Co			...	971	4.6B			
CoO, 298°K			888	780	...			
CoO, 78°K			942	751	5B approx.			
CoBr_2 Soln.			950	860	4.6B assumed			
$\text{CoBr}_2 \cdot 6\text{H}_2\text{O}$ Cryst.			910	775	4.6B assumed			
Co in MgO			960	833	...			

the quartet levels. This makes the experimental determination of the doublet levels difficult because they appear only as shoulders on more intensive absorptions. At 298°K the doublet transitions were so faint and poorly resolved that no attempt was made to determine a value of C .

The absorption of CoO at 78°K, which is now in the antiferromagnetic state, is given in Fig. 1. There has been a considerable sharpening of the absorptions and a drop in the optical density at all wavelengths. The entire spectrum has shifted towards shorter wavelengths. In addition it is seen that the main transition ${}^4F_1 \rightarrow {}^4F_1$ has become a double peak indicating a splitting of the upper 4F_1 level. CoO is known to undergo a tetragonal distortion on becoming antiferromagnetic.^{11,12} The addition to the dominant cubic potential of a crystal field term with tetragonal symmetry will cause a splitting of both the 4F_1 levels and of the 4F_2 level into two levels each. We believe that the appearance of the double peak in the ${}^4F_1 \rightarrow {}^4F_1$ transition and the additional structure in the ${}^4F_1 \rightarrow {}^4F_2$ transition found at 78°K is due to this tetragonal distortion. This is discussed in more detail later in this section.

The position of the transition from the ground 4F_1 level to the 4F_2 state has shifted from 7813 cm^{-1} to 8333 cm^{-1} at 78°K and the center of the absorption associated with the upper 4F_1 state has moved from 18 450 cm^{-1} to 18 520 cm^{-1} . The values of Dq and B which fit these new positions are $Dq=942 \text{ cm}^{-1}$ and $B=751 \text{ cm}^{-1}$. Using these values the 4A_2 level is calculated to lie at 17 757 cm^{-1} above the ground state.

At 78°K a number of shoulders appear in the absorption curve, some well defined while others are very vague although reproducible. We have determined the value of the parameter C which seems to correspond most closely to the positions of this additional structure. The value found was $C=5B$ in contrast to an estimate by Tanabe and Sugano of $C=4.6B$. In Table I the crystal field levels are listed and the observed and predicted absorptions neglecting both spin orbit coupling and the

tetragonal distortion of CoO below the Néel point. Leaving aside the upper two doublet states, the agreement is to within 5%.

Also listed in Table I are the results of Pappalardo¹³ for $\text{CoBr}_2 \cdot 6\text{H}_2\text{O}$ at 20°K and in solution at room temperature. The results obtained by Low¹⁴ for Co^{++} in MgO are also given as well as a comparison of Dq , B , and C for all of these cases including the free Co^{++} ion. The similarity in the optical absorption of Co^{++} in these various environments is evident. Pappalardo found a series of 8 absorptions lying between 19 745 cm^{-1} and 20 980 cm^{-1} which he assumes are to be identified with the upper 2F_1 level, and another series of 9 lines from 21 750 cm^{-1} to 24 375 cm^{-1} which he associates with the 2A_1 and still higher 2F_1 and 2F_2 levels. In this work a very well-defined absorption was found at 20 080 cm^{-1} which is undoubtedly due to the 2F_1 state. The two very weak absorptions at 20 060 and 21 010 cm^{-1} cannot be assigned with any certainty, which makes the agreement between theory and experiment at worst within 10% and at best within 5%.

The energy of the doublet states in the antiferromagnetic phase cannot be given accurately by crystal field theory which assumes that the environment of the ion is represented only by an electrostatic potential independent of the spin of the ion. This is true because the exchange or superexchange interactions of the Co^{++} with its surroundings, which is responsible for the antiferromagnetism, are certainly different for a Co^{++} with spin $\frac{3}{2}$ and a Co^{++} with spin $\frac{1}{2}$. Phenomenologically one should perhaps determine Dq , B , and C separately for the doublets.

Finally we take up the splitting observed in the ${}^4F_1 \rightarrow {}^4F_2$ and ${}^4F_1 \rightarrow {}^4F_1$ transitions. The ground state of Co^{++} in the cubic crystalline field being 4F_1 has a threefold orbital degeneracy. According to the Jahn Teller theorem this is an unstable situation and the crystal will spontaneously distort producing a splitting of the orbitally degenerate ground state and a crystal field level of lower energy. The deformation is halted because

¹¹ H. Rooksby and N. Tombs, *Nature* **167**, 364 (1950).

¹² S. Greenwald, *Acta Cryst.* **6**, 396 (1953).

¹³ R. Pappalardo (to be published).

¹⁴ W. Low, *Phys. Rev.* **109**, 256 (1958).

of the opposing increase in the elastic energy. Kanamori¹⁵ has examined a variety of contributions to the magnetoelastic energy in CoO and concludes that the mechanism cited above plays the dominant role in the deformation.

In order to have a rough idea of the size of the tetragonal crystalline field produced by the deformation, spin-orbit coupling was neglected, and following Abragam and Pryce¹⁶ the tetragonal field was expressed by

$$H'(2z^2 - x^2 - y^2) + I'(2z^4 - x^4 - y^4 + 12x^2y^2 - 6y^2z^2 - 6z^2x^2).$$

Values of $H = eH'\langle r^2 \rangle$ and $I = eI'\langle r^4 \rangle$ of 410 cm⁻¹ and 428 cm⁻¹, respectively were determined from the observed spectrum. Using these results, the splittings of the orbitally degenerate quartet states were calculated. The results are compared with the observed splittings in Table II.

The spin-orbit coupling parameter λ is -180 cm⁻¹ in the free Co⁺⁺ ion. Even allowing for a considerable reduction in λ for CoO, the effect of the tetragonal distortion will be of magnitude comparable to $\lambda\mathbf{L}\cdot\mathbf{S}$. Therefore, the values of H and I calculated here neglecting $\lambda\mathbf{L}\cdot\mathbf{S}$ represent only an upper limit to the strength of the tetragonal field.

Mn⁺⁺ IN A CUBIC FIELD

The energy level scheme for Mn⁺⁺ with configuration d^5 in a cubic crystal field and showing only the excited quartet states is given in Fig. 5. The energies of the 4F_1 and 4F_2 states, to which transitions are indicated in Fig. 5, are derived from the solutions of 3×3 secular

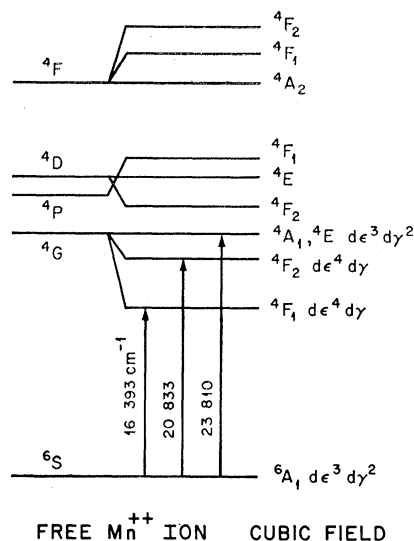


Fig. 5. Energy level scheme for the Mn⁺⁺ ion with d^5 configuration in a cubic crystal field. Observed transitions shown by arrows.

equations due to the interaction between states of 4F_1 or 4F_2 symmetry which arise from the 4G , 4P , or 4D , and 4F states of the free ion. The 4E energies are found from a 2×2 secular equation coming from the 4G and 4D free ion levels. The lowest eigenvalue of this 2×2 equation is $-25B+5C$ which turns out to be degenerate with the energy of the 4A_1 state. All of the secular equations are given by Tanabe and Sugano and are reproduced here in Eqs. (1), (2), and (3).

$${}^4F_1({}^4P, {}^4F, {}^4G) \begin{vmatrix} -10Dq-25B+6C-\lambda & -3\sqrt{2}B & C \\ -3\sqrt{2}B & -16B+7C-\lambda & -3\sqrt{2}B \\ C & -3\sqrt{2}B & 10Dq-25B+6C-\lambda \end{vmatrix} = 0, \quad (1)$$

$${}^4F_2({}^4F, {}^4G, {}^4D) \begin{vmatrix} -10Dq-17B+6C-\lambda & (\sqrt{6})B & 4B+C \\ (\sqrt{6})B & -22B+5C-\lambda & -(\sqrt{6})B \\ 4B+C & -(\sqrt{6})B & 10Dq-17B+6C-\lambda \end{vmatrix} = 0, \quad (2)$$

$${}^4E({}^4D, {}^4G) \begin{vmatrix} -22B+5C-\lambda & -2\sqrt{3}B \\ -2\sqrt{3}B & -21B+5C-\lambda \end{vmatrix} = 0. \quad (3)$$

The solutions of the cubic equations as a function of Dq , B , and C were kindly made available by Koster who with Heidt and Johnson have studied the optical ab-

TABLE II. Splittings of the orbitally degenerate quartet states in CoO in cm⁻¹.

State	(ground) 4F_1	4F_2	4F_1
Splitting (obs.)	...	1080	530
Splitting (calc.)	230	860	490

¹⁵ J. Kanamori, Progr. Theoret. Phys. (Kyoto) **17**, 197 (1957).

¹⁶ A. Abragam and M. H. L. Pryce, Proc. Roy. Soc. (London) **A206**, 173 (1951).

sorption of solutions of manganous perchlorate.¹⁷ Since there were no experimentally significant changes in the absorption of MnO between room temperature and 78°K, ($T_N=120^\circ\text{K}$), only one determination of Dq , B , and C was necessary. Due to the unavoidably thick single-crystal sample, 80 microns, only three absorptions were observable. Thus our only tests of the validity of crystal field theory are to compare the values found here for the parameters with those found in a case such as in reference 17 where the theory works well and secondly, to see whether the general features of the MnO spectrum are in accord with theoretical predictions.

¹⁷ Heidt, Koster, and Johnson, J. Am. Chem. Soc. **80**, 6471 (1958).

TABLE III. Values of Dq , B , and C for Mn^{++} for the indicated circumstances.

	Dq (cm^{-1})	B (cm^{-1})	C (cm^{-1})
Single-crystal MnO	979	786	3210
$Mn(ClO_4)_2$ Aq.	848	671	3710
Mn^{++} free	...	786	3790

Before turning to these comparisons it is to be noted that all transitions to the excited states of the d^5 configuration involve a change in multiplicity. This requires spin-dependent interactions which will break down the selection rule $\Delta S=0$. Spin-orbit and spin-spin coupling fulfill this need and one can find a detailed discussion of their role in the ground state of Mn^{++} by Watanabe.¹⁸

The values of the parameters Dq , B , and C which fit the three transitions indicated in Fig. 5 are listed in Table III and compared there with the results of Heidt, Koster, and Johnson and with the B and C values for the free Mn^{++} ion.

It will be noted that in Fig. 5 the energy separation of the ground 6A_1 state and the degenerate 4A_1 and 4E states is independent of the strength of the cubic field Dq . Furthermore, the ${}^6A_1-{}^4A_1$, 4E transition may be seen from Fig. 2 to be unusually sharp. A very plausible explanation of this is that fluctuations in the strength of the cubic field due to lattice vibrations will not lead to line broadening in such a transition but will contribute to the line width when the initial and final states have a different energy dependence on Dq . The fact that the values of Dq , B , and C seem to be reasonable in comparison with other cases and that an expected sharp transition occurs in the position indicated by the theory, i.e., after the ${}^6A_1-{}^4F_1$ and ${}^6A_1-{}^4F_2$ transitions, bears out the validity of crystal field theory for MnO.

THE ION-PHONON INTERACTION

In this section we briefly consider the coupling between the ions and the lattice and the mechanism underlying the optical transitions. In both MnO and CoO the paramagnetic ions lie at a center of inversion in both the paramagnetic and antiferromagnetic states. Also the initial and final crystal field levels in all observed transitions have even parity. Therefore, direct electric dipole transitions are forbidden. Tanabe and Sugano compare three possible mechanisms for the transitions; magnetic dipole, electric quadrupole, and a process first suggested by Van Vleck^{19,20} in which lattice

vibrations move the paramagnetic ion from the center of inversion symmetry thus admixing states of both parities into the crystal field levels. This process is shown diagrammatically in Fig. 6. Tanabe and Sugano estimate that the electric dipole-phonon process is roughly two orders of magnitude more likely than the other two mentioned. According to Liehr and Ballhausen's discussion²¹ of the electric dipole-phonon transitions, the absorption coefficient at the absorption peak should vary approximately as $\coth(h\nu_k/2kT)$, where $h\nu_k$ is the energy of the longitudinal optical phonon. This is found to give a good fit to the observed temperature dependence of the absorption coefficient

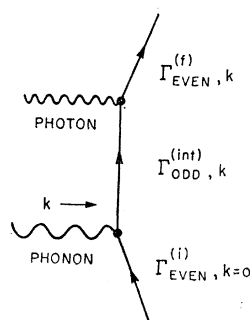


FIG. 6. Van Vleck mechanism for electric dipole transitions for crystal fields with inversion symmetry.

for the ${}^4F_1-{}^4F_1$ transition in CoO with $h\nu_k=0.1$ ev. This may be interpreted as a confirmation that the Van Vleck mechanism is responsible for the optical transitions in CoO. The temperature dependence of the absorption coefficient of MnO is not yet complete.

The excitation of the paramagnetic ions corresponds to the Frenkel exciton where the electron and hole are tightly bound to each other. Since the excitation can move through the lattice, the excited electronic states should be described in terms of excitation waves with corresponding exciton bands. The coupling to the phonons which plays a dominant role in making the optical transitions possible will also have the effect of allowing transitions from the initial state, which may be assumed to have $k=0$, to any k value of the exciton band. Therefore, the width of the absorption will be at least as wide as the exciton band width. On top of these considerations we must also consider the spin wave spectrum in the antiferromagnetic state. A detailed treatment of this interplay of phonons, excitation waves, spin waves, and photons will appear in a future publication.

¹⁸ H. Watanabe, Progr. Theoret. Phys. (Kyoto) **18**, 405 (1957).

¹⁹ J. H. Van Vleck, J. Phys. Chem. **41**, 64 (1937).

²⁰ J. H. Van Vleck, J. Chem. Phys. **7**, 72 (1939).

²¹ A. D. Liehr and C. J. Ballhausen, Phys. Rev. **106**, 1161 (1957).